Optical Engineering

SPIEDigitalLibrary.org/oe

Uniformity of image amplification by two-wave mixing in photorefractive crystals

Danyu Chen
Fengchun Tian
Youwen Hu
Ying Liu
Liang Han

SPIE

Uniformity of image amplification by two-wave mixing in photorefractive crystals

Danyu Chen, Fengchun Tian,* Youwen Hu, Ying Liu, and Liang Han
Chongqing University, College of Communication Engineering, Shazheng Street No. 174, Shapingba District, Chongqing 400030, China

Abstract. A model of two-wave mixing in the photorefractive crystal, which takes account of the difference in spatial frequency in a beam, has been built to study the uniformity of image amplification. Based on the theoretical analysis of the model, the gain distribution for each pixel in the signal beam has been obtained. It shows that the unevenness of the gain is induced by the difference in spatial frequency in the beam. The factors that impact on the uniformity of image amplification have been analyzed. As an example, the effects of these factors in a given photorefractive crystal have been studied through simulation. [DOI: 10.1117/1.OE.53.3.033106]

Keywords: two-wave mixing; photorefractive effect; light amplification; uniformity.

Paper 131691 received Nov. 4, 2013; revised manuscript received Dec. 25, 2013; accepted for publication Feb. 13, 2014; published online Mar. 21, 2014.

1 Introduction

Two-wave mixing, as an interesting phenomenon of great research and application value in nonlinear optics, has received growing interest in the past four decades. In a photorefractive crystal, two-wave mixing can be explained as the nonlinear interaction of intensity and phase between two incident beams through the photorefractive effect.[1–3] The diffusion effects in the crystal are not negligible, since there is a strong possibility that beam shape distortion will occur in a diffusion-dominated photorefractive material, and this has also been observed in the previous experimental results of volume holographic recording and reconstruction using a Fe-doped $LiNbO_3$ crystal.[4] Plenty of effective applications of two-wave mixing have been applied to different fields, such as real-time holography, self-pumped phase conjugation, coherent image amplification, optical storage, etc.[5–7] For real-time beam shaping, laser beam profile may be monitored during pulse duration, researchers suggested adaptive method, based on dynamic holographic gratings, recorded in photosensitive materials.[8]

As for two-dimensional (2-D) image amplification, it is a practical way to make use of photorefractive crystals in two-wave mixing arrangements because of the relative convenient operation and the potential for high gain.[9–11] To achieve high-quality image amplification, not only the value of gain needs to be considered but also the uniformity of the amplification for each pixel in the image, which takes account of the difference in spatial frequency in a beam. The gain nonuniformity will introduce serious wavefront distortion and apparent polarization state degradation to the output beam. Especially, the induced perturbation between the spatial intensity and phase of the beam, which increases rapidly with the propagation in nonlinear media, will cause small-scale self-focusing in the beam and even devastating damage to the elements in the light path. Therefore, it is of great significance to explore the uniformity of image amplification by two-wave mixing. However, most research on coherent image amplification by two-wave mixing in the previous literature only emphasized on the condition of a single spatial frequency.[1,12–15]

In this article, the uniformity of image amplification by two-wave mixing in photorefractive crystal, which takes the difference in spatial frequency in a beam into account, has been studied in detail.

2 Theoretical Analysis

The model of two-wave mixing in the previous literatures, which are concentrated on the situation for a single spatial frequency, has been presented in Fig. 1.

As seen in Fig. 1, the two beams I_1 and I_2 enter into a photorefractive crystal symmetrically. The interference intensity $I(x)$ and refractive index $n(x)$ distributing equations [10] can be expressed as

$$I(x) = I_0(1 + m\cos kx), \tag{1}$$

$$n(x) = n_0 + m\Delta n_s \cos(kx + \psi), \tag{2}$$

where $m = 2\sqrt{I_1 I_2}/I_1 + I_2$ is the intensity modulation depth; Δn_s is the saturation value of photoinduced refractive index change; k is the value of index gratings wave vector; ψ is the phase offset between the interference intensity pattern and refractive index gratings.

In order to study the uniformity of amplification by two-wave mixing in photorefractive crystal, a model that takes account of the difference in spatial frequency in a beam has been built. And the geometrical configuration has been presented in Fig. 2.

As seen in Fig. 2, C is the optical axis of the crystal, which is parallel to x-axis. Assuming the pump and signal beam, both of which are superposition of a series of plane waves, enter into the medium symmetrically with respect to the normal (z-axis) from the left side ($z = 0$). And both of them are s-polarized (electrical field vector is perpendicular to the incident plane). Sometimes, two lenses are being

*Address all correspondence to: Fengchun Tian, E-mail: fengchuntian@cqu.edu.cn

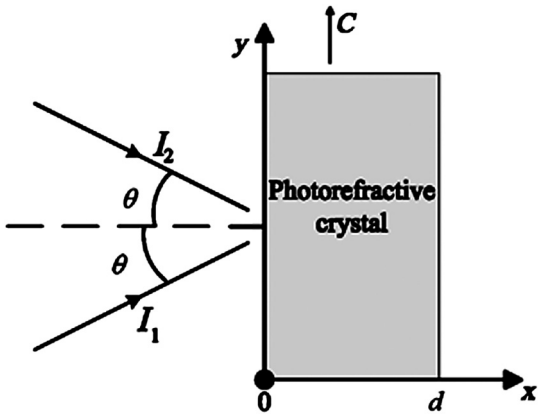

Fig. 1 Previous model of two-wave mixing. It is a geometrical configuration with regard to a single spatial frequency.

used to focus energy of the two beams to the crystal (Fourier plane of the lenses), the plane waves are converted to spherical waves. But, here we just consider the situation of plane wave incidence. The two beams couple with each other in the crystal, which leads to the amplification of the signal beam at the expense of the pump beam intensity decrease. For both the pump and signal beam, the optical field analytical expression on each pixel can be represented by $\mathbf{A}(p,q)\exp[\mathrm{i}(\omega t-\mathbf{a}(p,q)\cdot\mathbf{r})]$ and $\mathbf{B}(m,n)\exp[\mathrm{i}(\omega t-\mathbf{b}(m,n)\cdot\mathbf{r})]$; separately, where (p,q) indicates the spatial locations of light on individual pixel in the pump beam, and (m,n) similarly in the signal beam; $p=1,2,\ldots,P$; $q=1,2,\ldots,Q$; $m=1,2,\ldots,M$; $n=1,2,\ldots,N$; $\mathbf{a}(p,q)$ and $\mathbf{b}(m,n)$ are separately the wave vectors on each pixel in the pump and signal beam, which can be expressed with the coordinate system in Fig. 2.

To explore the gain distribution in the signal beam, the difference among incident angles for each pixel has been taken into account for both the pump and signal beam. As a small divergence angle will be induced with the spatial propagation in Gaussian beam shot from a laser,[16] the pump and signal waves span a rather small angular range, which results in different spatial frequencies in a beam. The offsets of the propagation direction on each pixel to the average propagation direction are represented by $\delta_p(p,q)$ and $\delta_s(m,n)$ separately for the pump and signal waves.

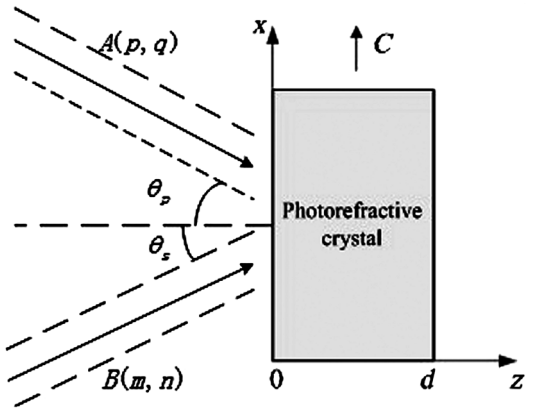

Fig. 2 Proposed model of two-wave mixing. It is a geometrical configuration in view of the different spatial frequencies in a beam.

Therefore, when entering into the crystal, the incident angle on each pixel in the pump and signal beam can be represented separately by $\alpha(p,q)=\theta_p+\delta_p(p,q)$ and $\beta(m,n)=\theta_s+\delta_s(m,n)$, where θ_p and θ_s indicate the average incident angle of the pump and signal beam, respectively. Ordinarily, $\theta_s=\theta_p=\theta$ is assumed.

As is known, the far-field small divergence angle δ of laser beams can be figured out by the formula[16]

$$2\delta=\frac{2\lambda}{\pi\omega_0},\omega_0=\sqrt{\frac{\lambda L}{2\pi}}, \tag{3}$$

where L is the resonant cavity length of the laser, λ is the wavelength of the beams. Consequently, for the pump and signal waves, $\delta_p(p,q)$ and $\delta_s(m,n)$ vary over a range of $\pm\delta$ separately, i.e., the incident angle on each pixel in the signal beam $\beta(m,n)$ range from $\theta-\delta$ to $\theta+\delta$.

The interference intensity of the pump and signal waves in the crystal, which has been deduced from Eq. (1), can be expressed as

$$\begin{aligned}I=I_0+\Bigg(&\frac{1}{2}\sum_{p=1}^{P}\sum_{q=1}^{Q}A(p,q)\sum_{m=1}^{M}\sum_{n=1}^{N}B^*(m,n)\\&\times\exp\{\mathrm{i}[\mathbf{a}(p,q)-\mathbf{b}(m,n)]\cdot\mathbf{r}\}\\&+\frac{1}{4}\sum_{\substack{p=1\\p\neq x}}^{P}\sum_{\substack{q=1\\q\neq y}}^{Q}A(p,q)\sum_{x=1}^{P}\sum_{y=1}^{Q}A^*(x,y)\\&\times\exp\{\mathrm{i}[\mathbf{a}(p,q)-\mathbf{a}(x,y)]\cdot\mathbf{r}\}\\&+\frac{1}{4}\sum_{\substack{m=1\\m\neq j}}^{M}\sum_{\substack{n=1\\n\neq k}}^{N}B(m,n)\sum_{j=1}^{M}\sum_{k=1}^{N}B^*(j,k)\\&\times\exp\{\mathrm{i}[\mathrm{b}(m,n)-\mathbf{b}(j,k)]\cdot\mathbf{r}\}\Bigg)+\mathrm{c.c.},\end{aligned} \tag{4}$$

where $I_0=\sum_{p=1}^{P}\sum_{q=1}^{Q}I_p(p,q;0)+\sum_{m=1}^{M}\sum_{n=1}^{N}I_s(m,n;0)$ is the total intensity of the incident pump and signal beam; c.c. indicates the complex conjugate of the previous term.

The charge carriers resulted from interference intensity pattern are liberated and redistribute themselves with the effect of drift or diffusion. A charge imbalance, which results in a modulated electric field, occurs and thereby, alters the spatial distribution of the refraction index in the crystal through the electro-optic effect.[17]

Since the angular range of the incident beam is much smaller than the average incident angle for both the pump and signal beam [i.e., $\delta_p(p,q)\ll\theta_p$ and $\delta_s(m,n)\ll\theta_s$], the interference between the pump waves, as well as that between the signal waves, will induce index gratings which are much weaker than those written by the interference between the pump and signal waves.[18] This is the scenario that can be approximately simplified as that, only the index gratings that written by the interference between the pump and signal waves make contribution to the energy transfer between the two beams.

A phase offset between the interference intensity pattern and the index gratings may exists in the crystal. When no external electric field is applied (i.e., diffusion is the dominated effect for the transport of the charge carriers), the phase

offset becomes $\pi/2$, in which case the energy transfer reaches its peak whereas the phase coupling disappears.[19,20] Therefore, based on Eq. (2), the refractive index distribution can then be approximated as

$$n = n_0 + \mathrm{i}\frac{n_1}{2I_0}\sum_{p=1}^{P}\sum_{q=1}^{Q}A(p,q)\sum_{m=1}^{M}\sum_{n=1}^{N}B^*(m,n) \times \exp[\mathrm{i}(\mathbf{a}(p,q)-\mathbf{b}(m,n))\cdot\mathbf{r}] + \text{c.c.}, \quad (5)$$

where n_0 is the refractive index of the crystal when no light is present; n_1 is the modulation factor of refractive index, which depends on the spacing and direction of the grating, as well as on the material properties of the crystal, e.g., the electro-optic coefficient. Equation (5) is solved for the steady state so that the amplitudes $A(p,q)$ and $B(m,n)$ are taken to be time independent.

With this and the slowly varying amplitude approximation,[21] Maxwell's scalar equations yield the following coupled amplitude equations

$$\frac{\mathrm{d}A(p,q;r)}{\mathrm{d}r} = -\frac{\gamma_p(p,q)}{I_0}\sum_{m=1}^{M}\sum_{n=1}^{N}|B(m,n;r)|^2A(p,q;r) - \frac{1}{2}\sigma A(p,q;r)p = 1,2,\ldots,P; \quad q = 1,2,\ldots,Q;\gamma_p(p,q) = \frac{\pi n_1}{\lambda\cos\alpha(p,q)}, \quad (6)$$

$$\frac{\mathrm{d}B(m,n;r)}{\mathrm{d}r} = \frac{\gamma_s(m,n)}{I_0}\sum_{p=1}^{P}\sum_{q=1}^{Q}|A(p,q;r)|^2B(m,n;r) - \frac{1}{2}\sigma B(m,n;r)m = 1,2,\ldots,M; \quad n = 1,2,\ldots,N;\gamma_s(m,n) = \frac{\pi n_1}{\lambda\cos\beta(m,n)}, \quad (7)$$

where σ is the absorption coefficient of the crystal, which is regulated by the wavelength of the incident beam.

Since the relation between the intensities and amplitudes of the incident beams are $I_p(p,q;r) = |A(p,q;r)|^2$ and $I_s(m,n;r) = |B(m,n;r)|^2$, the coupled intensity equations are given by

$$\frac{\mathrm{d}I_p(p,q;r)}{\mathrm{d}r} = -\frac{\Gamma_p(p,q)}{I_0}\sum_{m=1}^{M}\sum_{n=1}^{N}I_s(m,n;r)I_p(p,q;r) - \sigma I_p(p,q;r) \quad p = 1,2,\ldots,P; \quad q = 1,2,\ldots,Q; \quad \Gamma_p(p,q) = 2\gamma_p(p,q), \quad (8)$$

$$\frac{\mathrm{d}I_s(m,n;r)}{\mathrm{d}r} = \frac{\Gamma_s(m,n)}{I_0}\sum_{p=1}^{P}\sum_{q=1}^{Q}I_p(p,q;r)I_s(m,n;r) - \sigma I_s(m,n;r)m = 1,2,\ldots,M; \quad n = 1,2,\ldots,N; \quad \Gamma_s(m,n) = 2\gamma_s(m,n). \quad (9)$$

In the assumed diffusion driven scenario, the phases of the beams are decoupled so that the intensity Eqs. (8) and (9) describe the two-wave mixing process completely.

With Eqs. (8) and (9), one can integrate to yield the intensity versus effectively acting distance r on each pixel in the signal beam, which can be normalized by the initial intensity as

$$\frac{I_s(m,n;r)}{I_s(m,n;0)} = \frac{1+h}{1+he^{-\Gamma_s(m,n)r}}e^{-\sigma r}, \quad h = \frac{\sum_{p=1}^{P}\sum_{q=1}^{Q}I_p(p,q;0)}{\sum_{m=1}^{M}\sum_{n=1}^{N}I_s(m,n;0)}. \quad (10)$$

Therefore, the gain, which is defined as the intensity ratio of the output signal wave in the presence of a pump beam to that in the absence of a pump beam, can be given by

$$G(m,n) = \frac{I_s(m,n;l)}{I_s(m,n;0)} = \frac{1+h}{1+he^{-\Gamma_s(m,n)l}}e^{-\sigma l}, \quad l = \frac{d}{\cos\beta_i(m,n)}, \quad (11)$$

where d is the thickness of the crystal, $\beta_i(m,n)$ is the angle between the propagation direction and the normal (z-axis) on each pixel in the signal beam inside the crystal, and l is the effective interaction length on individual pixel in the signal beam.

To calculate the gain, the expression of intensity coupling coefficient $\Gamma_s(m,n)$,[22] presented below, can be inserted into Eq. (11):

$$\Gamma_s(m,n) = \frac{A\sin\beta(m,n)}{1+B^{-2}\sin^2\beta(m,n)}\cdot\frac{\cos 2\beta_i(m,n)}{\cos\beta_i(m,n)}. \quad (12)$$

In Eq. (12), the related parameters are included in coefficients A and B, which can be given by

$$A = \gamma_{\mathrm{eff}}\xi(K)\frac{8\pi^2n^3k_BT}{e\lambda^2}, \quad (13)$$

$$B = \left(\frac{N_{\mathrm{eff}}}{\varepsilon\varepsilon_0k_BT}\right)^{1/2}\cdot\frac{e\lambda}{4\pi}, \quad (14)$$

where γ_{eff} is the effective electric–optic coefficient; n is the refractive index; $\xi(K)$ is the recombination constant, which is fixed when the value of $k = 2\pi/\lambda$ is set; N_{eff} is the effective charge density, which is regulated by the wavelength of the incident beams; k_B is the Boltzmann constant; T is the absolute temperature; e is the charge on the electron; λ is the wavelength of the incident beams.

According to the analysis above, the gain nonuniformity in the signal beam, which indicates the unevenness for image amplification, is induced by the difference in spatial frequency in the beam. As seen in Eqs. (11)–(14), the factors, which impact on the uniformity of amplification in the signal beam, are the crystal thickness d, the incident angle $\beta(m,n)$, and the wavelength λ.

3 Simulation and Discussion

To explore the effects of these factors on the uniformity of amplification in the signal beam, which loads a 2-D image, one can vary the average incident angle θ, the crystal thickness d and the wavelength of incident beam λ, respectively, and observe the behavior of the gain.

The nonuniformity of gain can be measured with the relative standard deviation $\gamma = \mathrm{SD}/\mathrm{AVG}$. Here, AVG and SD are the mean value and standard deviation of the gain in the signal image beam, respectively. The gain nonuniformity is negligible compared with the value of gain when γ reaches a low enough value. The usual requirement is $\gamma = 1\%$.

In this article, the numerical simulation for two-wave mixing is based on the model analyzed above. Assuming the signal beam and the pump beam are split from a laser beam at a ratio of 1:1120. Then, the two of them recombines at a photorefractive $\mathrm{Fe}(0.04\ \mathrm{wt}\%):\mathrm{Ce}(0.1\ \mathrm{wt}\%):\mathrm{LiNbO_3}$ crystal from the same side with the average incident angle $\theta_s = \theta_p = \theta$. Three scenarios with different wavelengths have been analyzed to obtain the gain distribution in the signal image beam.

3.1 *Argon Laser at* $\lambda = 488$ nm

In the first scenario, the light source is an argon laser with a cavity length of $L = 150$ cm operating at wavelength of 488 nm, in which case the crystal has the parameters of $\sigma = 21.2\ \mathrm{cm}^{-1}$ and $N_{\mathrm{eff}} = 2.9 \times 10^{15}\ \mathrm{cm}^{-3}$ according to Ref. 22. Substituting λ and L into Eq. (3) yields the far-field small divergence angle of the laser beam: $\delta = 0.026075$ deg. Arbitrary values within $\pm\delta$ range can be assigned to $\delta_s(m,n)$, the offset of the propagation direction on individual pixel to the average propagation direction in the signal image beam, to work out the gain with Eqs. (11)–(14).

Computer-generated plots of the main value of gain AVG and nonuniformity parameter γ versus average incident angle θ and crystal thickness d have been presented in Fig. 3. The conditions that the value of gain is <0 dB (i.e., the intensity of the signal image wave is reduced in the crystal[23]) have been ignored.

As seen in Fig. 3(a), for different values of d, AVG represents difference in fluctuating amplitude while similar in trend of variation with the change of θ. That is, the effects of angle θ on AVG are similar for different values of d. The value of AVG increases with the increasing of θ, first reaches a maximum, then decreases. For each value of d, AVG reaches its maximum with a same fixed value of θ, i.e., 17 deg. The similar trend of variation can be seen in Fig. 3(b) for value of γ. For arbitrary value of d, γ reaches its minimum with the same value of $\theta = 17$ deg, and this is due to the minimal gradient of AVG. When the average incident angle θ is 17 deg, the incident angle of signal and pump beam on each pixel are around the value of 17 deg, which leads to a minimal fluctuation of AVG. As for this, the image can achieve the maximum gain and the highest level of amplification uniformity when the incident angle of beams is set as 17 deg.

The values of AVG, SD, and γ versus d for the optimal average incident angle $\theta_{\mathrm{opt}} = 17$ deg are presented in Fig. 4. The situation for $d > 0.33$ cm should be ignored due to its reduction of signal wave intensity in the crystal. Within the 0- to 0.33-cm range of d, γ increases with the increasing d,

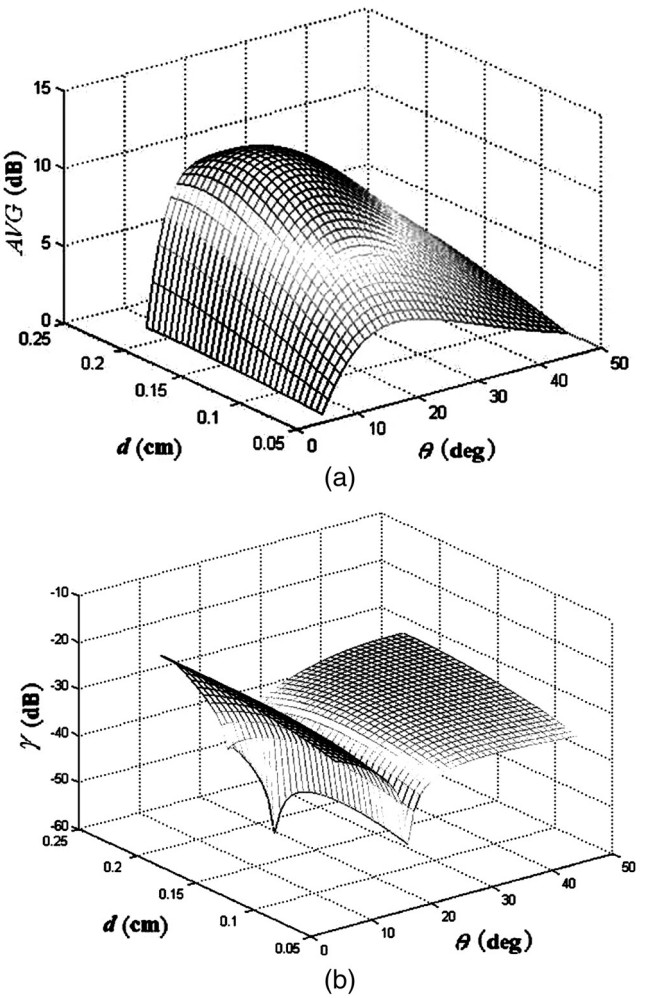

Fig. 3 Values of (a) main value of gain AVG and (b) nonuniformity parameter γ versus average incident angle θ and crystal thickness d, respectively, with $\lambda = 488$ nm.

then decreases to a minimum and afterward increases again. Particularly, the optimal thickness of the crystal d_{opt}, in which case γ reaches its minimum 0.00016%, is turned out to be 0.17 cm. Moreover, the maximum gain has been reached with $d = 0.17$ cm simultaneously.

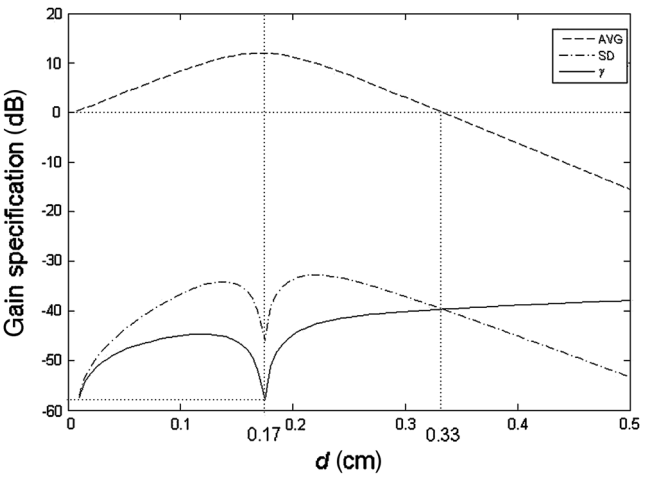

Fig. 4 Values of AVG, SD, and γ versus crystal thickness d for optimal average incident angle $\theta_{\mathrm{opt}} = 17$ deg with $\lambda = 488$ nm.

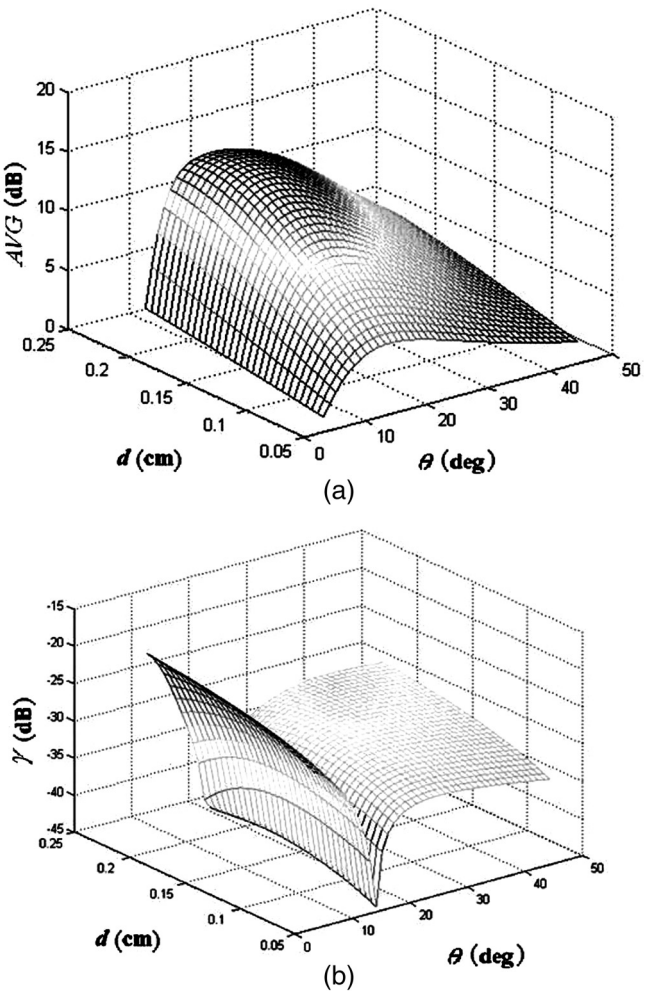

Fig. 5 Values of (a) main value of gain AVG and (b) nonuniformity parameter γ versus average incident angle θ and crystal thickness d, respectively, with $\lambda = 514.5$ nm.

3.2 *Argon Laser at* λ=514.5 nm

The second scenario is that the operating wavelength of the argon laser used in the first scenario is changed to 514.5 nm, in which case the crystal has the parameters of $\sigma = 16.2\ \text{cm}^{-1}$ and $N_{\text{eff}} = 1.9 \times 10^{15}\ \text{cm}^{-3}$ according to Ref. 22. What is more, the far-field small divergence angle of the laser beam is turned into $\delta = 0.026774$ deg.

Substituting σ, N_{eff}, and δ into the simulation carried on in the first scenario yields the gain distribution for each pixel in the signal image beam. The values of AVG and γ versus angle θ and d are shown in Fig. 5.

According to the results, the phenomenon that AVG and γ represent difference in fluctuating amplitude while similar in trend of variation with the change of θ for arbitrary value of d, is the same as that seen in the first scenario. The optimal average incident angle θ_{opt}, which will guarantee the maximum gain and the highest level of amplification uniformity regardless of the value of d, is appeared to be 15 deg.

Simulation results of AVG, SD, and γ versus d for θ_{opt} are presented in Fig. 6. Within the 0 to 0.43 cm range of d, γ increases with the increasing d, then basically remain unchanged. Since the signal beam has not been amplified when the gain is <0 dB, the situation with $d > 0.43$ cm should be ignored.

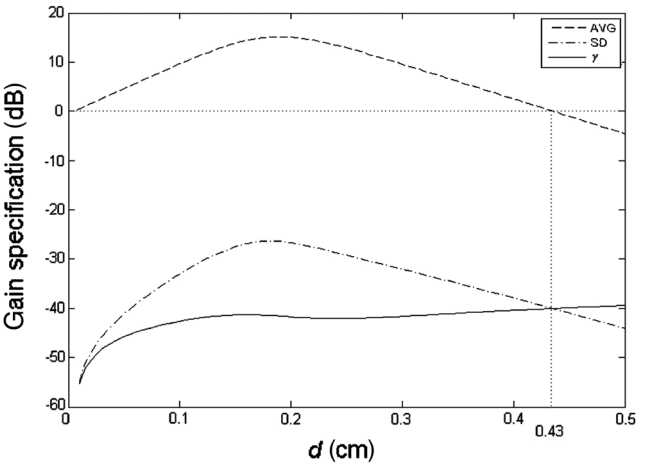

Fig. 6 Values of AVG, SD, and γ versus crystal thickness d for optimal average incident angle $\theta_{\text{opt}} = 15$ deg with $\lambda = 514.5$ nm.

3.3 *He–Ne Laser at* $\lambda = 632.8$ nm

The last scenario is that, the argon laser used in the first scenario is changed for a He–Ne laser with a cavity length of $L = 30$ cm at wavelength 632.8 nm, in which case the crystal has the parameters of $\sigma = 0.7\ \text{cm}^{-1}$ and

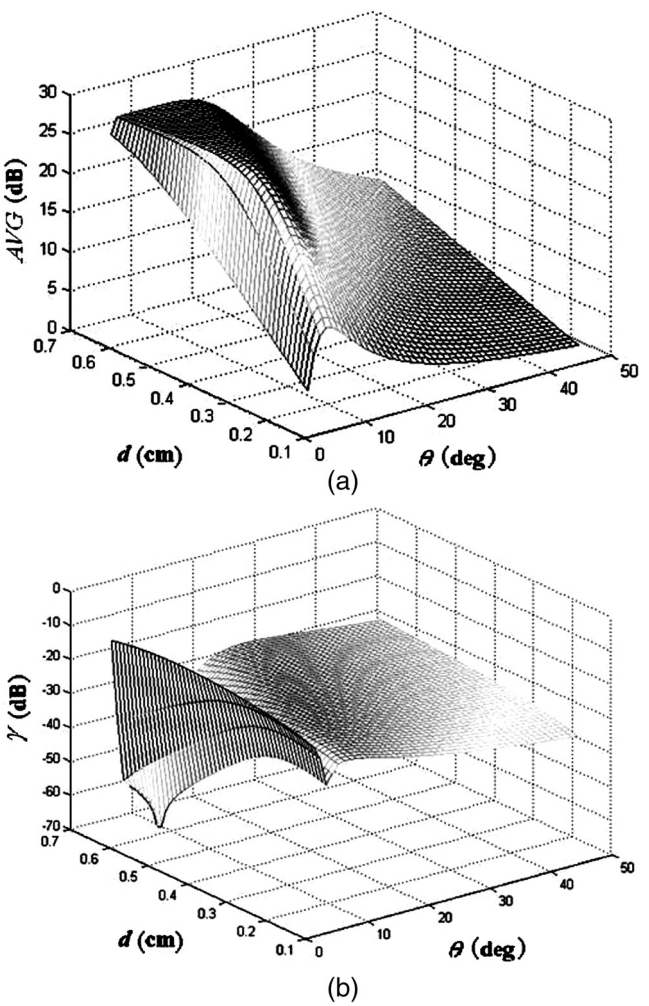

Fig. 7 Values of (a) main value of gain AVG and (b) nonuniformity parameter γ versus average incident angle θ and crystal thickness d, respectively, with $\lambda = 632.8$ nm.

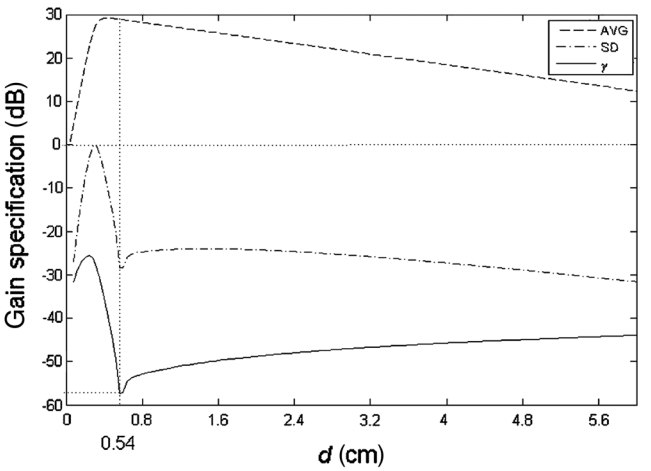

Fig. 8 Values of AVG, SD, and γ versus crystal thickness d for optimal average incident angle $\theta_{opt} = 4$ deg with $\lambda = 632.8$ nm.

$N_{eff} = 0.1 \times 10^{15}$ cm^{-3}. Besides, the far-field small divergence angle of the laser beam is turned out to be $\delta = 0.066395$ deg.

Similarly, bring σ, N_{eff}, and δ into the simulation carried on in the first scenario yields the gain distribution on each pixel in the output signal beam. The results of AVG and γ with varying angle θ and d are presented in Fig. 7. Note that the fluctuation amplitude of γ is larger than that in the previous two scenarios. The optimal average incident angle θ_{opt} is 4 deg.

The values of AVG, SD, and γ versus d for θ_{opt} have been presented in Fig. 8. γ increases with the increasing d, then decreases to a minimum and afterward increases again. The minimum value of γ (0.000184%) can be reached with $d_{opt} = 0.54$ cm.

By comparing the three scenarios above, the influence of the wavelength on the uniformity of image amplification can be observed. For different wavelengths of the incident beams, the values of γ fluctuate within different ranges and the optimal values of nonuniformity that can be reached are different.

4 Conclusions

In short, to explore the uniformity of image amplification by two-wave mixing in photorefractive crystals, a model in view of different spatial frequency in a beam has been built. According to the gain of signal beam deduced from the model, it is the difference in spatial frequency attributed to different incident angle on each pixel in the beam that induces the unevenness of image amplification. It has been proved that the factors which impact on the uniformity of image amplification are: the thickness of photorefractive crystal, the incident angle on each pixel in signal image beam, and the wavelength of incident beams. As an example, the effects of these factors in photorefractive $Fe(0.04\ wt\%):Ce(0.1\ wt\%):LiNbO_3$ crystal have been researched through simulation. It turns out that a considerable nonuniformity of $\gamma = 0.00016\%$ can be reached when the wavelength of the incident beam is 488 nm (at $\theta = 17$ deg, $d = 0.17$ cm).

Acknowledgments

This work was supported by the National Natural Science Foundation of China (No. 61071190, No. 61171158) and the Fundamental Research Funds for the Central Universities of China (No. CDJZR12160010).

References

1. N. V. Kukhrarev et al., "Holographic storage in electro-optic crystals. I. Steady state," *Ferroelectrics* **22**(1), 949–953 (1978).
2. M. C. Søren et al., "Two-wave mixing in a broad-area semiconductor amplifier," *Opt. Express* **14**(25), 12373–12379 (2006).10.5772/8665
3. M. C. Søren et al., "Nonlinear gain amplification due to two-wave mixing in a broad-area semiconductor amplifier with moving gratings," *Opt. Express* **16**(8), 5565–5571 (2008).
4. P. P. Banerjee et al., "Volume holographic recording and readout for 90-deg geometry," *Opt. Eng.* **43**(9), 2053–2060 (2004).
5. P. Günter and J. P. Huignard, *Photorefractive Materials and their Applications. I*, Springer-Verlag, Berlin (1987).
6. P. Günter and J. P. Huignard, *Photorefractive Materials and their Applications. II*, Springer-Verlag, Berlin (1989).
7. N. Katyal et al., "The influence of pump beam polarization on the signal beam, in TWM in photorefractive crystals: transmission geometry," *Optik* **122**(3), 207–210 (2011).
8. N. Kukhtarev et al., "Laser beam shaping by holographic optical elements," *Proc. SPIE* **5257**, 152–162 (2003).
9. N. V. Kukhrarev et al., "Holographic storage in electro-optic crystals. II. beam coupling-light amplification," *Ferroelectrics* **22**(1), 961–964 (1978).
10. J. P. Huignard and A. Marrakchi, "Coherent signal beam amplification in two-wave mixing experiments with photorefractive $Bi_{12}SiO_{20}$ crystals," *Opt. Commun.* **38**(4), 249–254 (1981).
11. Y. Fainman, E. Klancnik, and S. H. Lee, "Optimal coherent image amplification by two-wave coupling in photorefractive $BaTiO_3$," *Opt. Eng.* **25**(2), 228–234 (1986).
12. P. Tayebati and D. Mahgerefteh, "Theory of the photorefractive effect for $Bi_{12}SiO_{20}$ and $BaTiO_3$ with shallow traps," *J. Opt. Soc. Am. B* **8**(5), 1053–1064 (1991).
13. M. H. Garett et al., "High beam-coupling gain and deep- and shallow-trap effects in cobalt-doped barium titanate," *J. Opt. Soc. Am. B* **9**(8), 1407–1415 (1992).
14. K. Buse et al., "Photorefractive properties of tetragonal crystals and explanation by the three-valence charge-transport model," *J. Opt. Soc. Am. B* **13**(11), 2644–2651 (1996).
15. B. Peng et al., "Two-wave mixing of ion-implanted photorefractive waveguides in near-stoichiometric $Fe:LiNbO_3$ crystals," *Opt. Mater.* **33**(6), 773–776 (2011).
16. J. Chen, *Principle and Application of Laser*, T. Han, Ed., Publishing House of Electronics Industry, Beijing (2004).
17. P. G. Kazansky et al., "Pockels effect in thermally poled silica optical fibers," *Electron. Lett.* **31**(1), 62–65 (1995).
18. D. Z. Anderson and R. Saxena, "Theory of multimode operation of a unidirectional ring oscillator having photorefractive gain: weak field limit," *J. Opt. Soc. Am. B.* **4**(2), 164–176 (1987).
19. M. Chi, J. P. Huignard, and P. M. Petersen, "A general theory of two-wave mixing in nonlinear media," *J. Opt. Soc. Am. B* **26**(8), 1578–1584 (2009).
20. N. Koukourakis et al., "Photorefractive two-wave mixing for image amplification in digital holography," *Opt. Express* **19**(22), 22004–22023 (2011).
21. Z. Y. Li, B. Y. Gu, and G. Z. Yang, "Slowly varying amplitude approximation appraised by transfer-matrix approach," *Phys. Rev. B* **60**(15), 10644–10647 (1999).
22. C. Yang et al., *Photorefractive Nonliear Optical Materials:LiNbO3 Crystals*, J. Yang, Ed., Science Press, Beijing (2009).
23. T. K. Yadav, M. K. Maurya, and R. A. Yadav, "Effect of photoconductivity and oscillation frequency shift on the signal beam intensity in two beam coupling in photorefractive materials," *Optik* **122**(18), 1607–1614 (2011).

Danyu Chen received her BS degree in communication engineering from PLA Information Engineering University, Zhengzhou, China, in 2011. She is now a MS candidate in the College of Communication Engineering, Chongqing University, Chongqing, China. Her research focuses on optical information processing and image processing systems.

Fengchun Tian received his BE, ME, and DE degrees in radio engineering, biomedical instruments and engineering, theoretical electric engineering from Chongqing University, Chongqing, P.R. China, in 1984, 1986, and 1996, respectively. Since 1984, he has been working in Chongqing University as a teacher. Since 2007, he is also an

adjunct professor in the University of Guelph, Canada. His current research interests are image processing (including optical image and video processing), biomedical and modern signal processing technology.

Youwen Hu received his BS degree in telecommunication engineering from Chongqing University, Chongqing, China, in 2004. He received his MS degree in signal and information processing in Chongqing University, Chongqing, China. He is now a PhD candidate at Chongqing University. His research interests are adaptive optics, optical negative feedback system, and optical information processing.

Ying Liu received her BS degree in communication engineering from Qingdao University of Science and Technology, Qingdao, China, in 2012. Now, she is a graduate student in Chongqing University, Chongqing, China. Her research focuses on the optical image processing.

Liang Han received her MS degree in communication and information systems in 2004 and her PhD degree in circuits and systems in 2008 from the College of Communication Engineering, Chongqing University, Chongqing, China. In 1997, he joined Chongqing University, where he is currently an associate professor in the College of Communication Engineering. His research focuses on imaging processing, especially in multiresolution analysis and its optical implementation method, image fusion, image denoising, and weak signal extraction methods.